CLAS Data Analysis Proposal
The Photoproduction of $\phi(1020)$ Mesons from Hydrogen and Deuterium

H. Gao (Spokesperson),J. Adkins, W. Chen, D. Dutta, K. Kramer,W. Xu
Triangle Universities Nuclear Laboratory and Duke University

D. Tedeschi (Spokesperson), M. Paolone
University of South Carolina

K. Hicks, T. Mibe
Ohio University

S. Stepanyan
Thomas Jefferson National Accelerator Facility

June 16, 2005

Abstract

We propose a study of the production of $\phi(1020)$ mesons from hydrogen and deuterium using the CLAS g10 (deuterium) and g11 (hydrogen) data sets. This analysis will cover a photon energy range from the reaction threshold to 3.6 GeV; and the large solid angle coverage of CLAS will allow the detailed study of the production of $\phi(1020)$ mesons. The g11 data analysis will address outstanding questions regarding the photon-proton interaction. The g10 data analysis will study the coherent production from the deuterium nucleus and provide a separation of the iso-vector and iso-scalar amplitudes. Additionally, sub-threshold production of $\phi(1020)$ mesons from nucleons in deuterium will be measured to set a baseline for future searches for a ϕ-N bound state in subthreshold kinematics using nuclear targets.

1 Introduction

Quantum Chromodynamics (QCD) is the accepted theory of the strong interaction in terms of quark and gluon degrees of freedom. QCD is experimentally well tested in the extremely high energy regime. The perturbative QCD (pQCD) approach, which works successfully in the high energy regime, is not applicable in the relatively low energy, or confinement region. As such our knowledge of confinement and the structure of matter in terms of the underlying QCD degrees of freedom is rather poor because of our inability to solve QCD analytically. While lattice QCD is promising, its predictive power at the present time is still limited by computer performance and other technical issues, and this situation will likely remain in the foreseeable future. Therefore, experiments which test various QCD inspired models are essential in improving our knowledge of QCD in the confinement region. In the very low energy region, chiral perturbation theory, an effective theory based on the chiral symmetry (up and down quark masses very close to zero) of QCD is extremely important and productive. Heavy quark symmetry [1] in the strong interaction, discovered by Isgur and Wise, has important implications for describing the spectrum of particles containing a single heavy quark and their decays. The strange quark is rather unique in QCD being neither as light as the up/down quark nor as heavy as the charm quark, which makes the treatment of it rather difficult in various approaches. But the importance of the strange quark in the structure of nucleon, i.e. in the structure of matter is undebatable.

Reactions that involve ϕ meson production are sensitive to the degrees of freedom chosen to describe the reaction (nucleons and mesons vs. quarks and gluons), thus they are a good test of the transition from the non-perturbative to perturbative regime of quantum chromodynamics (QCD). For example, recent photoproduction data from CLAS has shown that at large momentum transfer the language of vector dominance - pomerons interacting with nucleons - must be replaced by gluons interacting with quarks.[2]

The following sections propose analyses of ϕ meson production from hydrogen and deuterium to investigate new production mechanisms, coherent production, and exotic $\phi - N$ bound states.

2 Production from Hydrogen

Early photoproduction measurements of ϕ-mesons are consistent with diffractive production via pomeron exchange as the dominant mechanism.[3] The differential cross sections for this reaction are forward peaked and vary slowly with energy away from threshold. [4, 5, 6] In addition, early polarization data agree with the predictions of the vector dominance model in which an $s\overline{s}$ pair is produced by the transformation of the incoming photon.[7, 8] Theoretical predictions [9, 10] and new data from the CLAS,[11] LEPS,[12] and SAPHIR[13] collaborations indicate that there is much more to learn

from this reaction.

The differential cross section for the photoproduction of the $\phi(1020)$ near threshold ($E_\gamma = 1.57GeV$) is predicted to be sensitive to production mechanisms other than diffraction. Presented in figure 1 are CLAS g1c data using unpolarized photons from threshold up to $E_\gamma = 2.4$ GeV and covering a range in momentum transfer up to $|t| = 1.6$ (GeV/c)^2. The error bars on the CLAS data include statistics from the data and Monte Carlo.

The data begin to depart from an exponential fall off around a momentum transfer of $t = 1.0$ $(GeV/c)^2$. The rise at large-t as predicted by the regge model of Laget is not expected to occur at such low photon energies.[14] This discrepancy can be accounted for by other photoproduction models that include s-channel (and u-channel) mechanisms such as phi-knock out or resonance coupling. [9, 10] Additionally, there may be experimental explanations for the rise such as background coming from $a0/f0(980)$ or $\Lambda(1520)$ production that is not accounted for.

The forward cross section near threshold is predicted to be sensitive to production processes involving glueballs or OZI evading mechanisms.[15, 9, 16] The signature of such mechanisms in the cross section is a departure from the smooth diffractive evolution as a function of photon energy. Shown in figure 2 are the cross section and slope data as a function of energy. The g1c data have qualitative agreement with the SAPHIR and LEPS data. The CLAS g1c and LEPS data seem to peak around 2 GeV while the SAPHIR data do not indicate a peak. The smooth solid curve include only diffractive contributions. The new data near threshold indicate a possible structure around E_γ of 2 GeV, yet a definitive interpretation of the data is precluded at this time. Analysis of the forward cross section with the new, high statistics g11 data set can proved the complete coverage in energy, from threshold to $3.6GeV$ that is needed to support or refute these alternate interpretations.

The analysis of the decay angular distribution of the the ϕ meson will also bring additional understanding of the reaction mechanism. Figure 3 shows the polar and azimuthal distributions in the Gottfried-Jackson frame. For unpolarized photons interacting via diffraction, the azimuthal distribution is expected to be flat. The CLAS g1c data show a $cos(2\phi)$ modulation. This behavior is also seen by SAPHIR for unpolarized photons[13] and is an indication that mechanisms other than diffractive pomeron exchange contribute the the phi production process near threshold.

3 Coherent ϕ Photoproduction on Deuterium

Precise knowledge of vector meson-nucleon cross sections are relevant for the investigation of hadron production processes. Despite the long history of experimental studies [3] the ϕ-nucleon cross section is not known to satisfactory accuracy. The ϕ-nucleon cross section is determined to be 7.7-8.7 mb from the ϕ photoproduction cross section on the proton at $E_\gamma = 6.4 - 9.0$ GeV [17]. This cross section is smaller than the quark model

prediction of 13.0±1.5 mb based on kaon-nucleon, pion-nucleon cross sections. However, a definitive statement requires more precise data.

Recently, LEPS reported much larger ϕ-nucleon cross section in the nuclear medium (35^{+17}_{-11} mb) from the A-dependence of the ϕ photoproducion yield on Li, C, Al, and Cu nuclei near the threshold ($E_\gamma = 1.5 - 2.4$ GeV) [18]. This result motivated the suggestion that the ϕ meson property is modified in the nuclear medium [19]. However, the ϕ-nucleon cross section is not necessarily independent of the energy of the ϕ-nucleon system. There is no measurement of the ϕ-nucleon cross section in free space near the threshold. As discussed in the previous section, the cross sections of ϕ photoproduction on the proton are not well determined near the threshold and might have a possible anomalous structure which could give rise to a larger ϕ-nucleon cross section. Therefore, new data on the ϕ-nucleon cross section near the threshold are desired to interpret the difference in the ϕ-nucleon cross sections reported in Ref. [17] and Ref. [18].

Frankfurt *et al.* [20] suggested that coherent vector meson photoproduction on the deuteron is sensitive to the interaction cross section between vector meson and nucleon. The reaction is described by the single and double scattering processes. Schematic diagrams are shown in Fig. 4. In the single scattering process, only one of the nucleons in deuteron participates in the reaction (Fig. 4(a)). The double scattering process involves re-scattering as depicted in Fig. 4(b), where interaction cross section can be studied via the re-scattering process.

The t dependence of the single scattering process will follow the deuteron form factor which is strongly forward peaked. On the other hand, the t dependence of the double scattering process is expected to have a less steep slope because the momentum transfer is shared between both the interacting nucleons. Frankfurt *et al.* demonstrated that the t distribution for the coherent ρ photoproduction is well described by the single and double scattering processes [20] (see Fig. 5). As seen in Fig. 5, differential cross sections at large |t| are entirely dominated by the double scattering process. It was shown that the differential cross section at large |t| for the coherent ϕ photoproduction from deuteron is sensitive to the ϕ-nucleon cross section [20]. However, only one measurement on deuteron exists and the photon energy region is $E_\gamma = 6.4 - 9.0$ GeV [23]. Furthermore, no t distribution is reported and no separation of incoherent process is made. The proposed g10 analysis will identify the coherent process unambiguously (see analysis section) and will provide the first result of the t distribution for the coherent ϕ photoproduction on deuteron.

In connection with the hydrogen data analysis, the analysis of coherent ϕ photoproduction on deuteron provides additional information on the dynamics of ϕ photoproduction. Since the deuteron is an iso-scalar particle, contributions from t-channel iso-vector exchange (i.e. π-meson exchange) are eliminated from possible reaction diagrams in the coherent ϕ photoproduction on deuteron. Note that the π-meson exchange contribution in the ϕ photoproduction on proton is expected to increase near the production threshold [9, 15]. Figure 6 shows theoretical predictions for the differential cross sections on

the proton and the deuteron at $E_\gamma = 2.2$ GeV [24]. There is no π-meson exchange contribution to the coherent production from deuteron. Therefore, the comparison of cross sections between the coherent ϕ production on deuteron and ϕ production on proton will identify the iso-vector exchange contribution in the ϕ photoproduction, and will also allow the extraction of the contribution from the iso-scalar part of the production process.

4 Exotic ϕ-N bound state and subthreshold ϕ photoproduction

It has been suggested[26] that the QCD van der Waals interaction, mediated by multigluon exchanges, is dominant when the interacting two color singlet hadrons have no common quarks. In fact, the QCD van der Waals interaction is enhanced at low velocity as has been shown by Luke, Manohar, and Savage[27]. This finding supports the prediction that a nuclear-bound quarkonium can be produced in charm production reactions at threshold, and the interpretation that the structures seen in $s^{10}d\sigma/dt(pp \to pp)$ and the A_{NN} spin correlation at $\sqrt{s} \sim 5$ GeV and large cm angles [28] can be attributed to $c\bar{c}uuduud$ resonant states[29]. If these interpretations are correct, then analogous effects could also be expected at the strangeness threshold.

Brodsky, Schmidt, and de Téramond [26] investigated the nuclear-bound quarkonium state using a non-relativistic Yukawa type attractive potential $V_{(Q\bar{Q})A} = -\alpha e^{-\mu r}/r$ characterizing the QCD van der Waals interaction. They determined the α and μ constants using the phenomenological model of high-energy Pomeron interactions developed by Donnachie and Landshoff [30]. Using a variational wave function $\Psi(r) = (\gamma^3/\pi)^{1/2}e^{-\gamma r}$, they predicted bound states of η_c with ^{3}He and heavier nuclei. Their prediction was confirmed by Wasson [31] using a more realistic $V_{(Q\bar{Q})A}$ potential taking into account the nucleon distribution inside the nucleus.

Similarly, one expects the attractive QCD van der Waals force dominates the ϕ-N interaction since the ϕ meson is almost a pure $s\bar{s}$ state. It is possible that a ϕ-N bound state or resonant state can be formed in some reactions. In photoproduction of ϕ meson from a proton target above threshold, the formation of a bound ϕ-N state is not likely because of the momentum mismatch between the ϕ and the recoil proton. As such, no experimental evidence exists on the formation of the ϕ-N bound state up to now. On the other hand, such a ϕ-N bound state could be formed inside a nucleus.

Using the variational method and following Ref.[26] to assume $V_{(s\bar{s}),N} = -\alpha e^{\mu r}/r$, Gao, Lee and Marinov [33] find that a bound state of ϕ-N is possible with $\alpha = 1.25$ and $\mu = 0.6$ GeV. The binding energy obtained is 1.8 MeV. Their results should be compared with $\alpha = 0.6$ and $\mu = 0.6$ GeV determined by Brodsky, Schmidt, and de Téramond [26] for the $c\bar{c}$ quarkonium. The interaction is expected to be enhanced by $(m_c/m_s)^3$, i.e., $q\bar{q}$ separation cubed, from $c\bar{c}$ to $s\bar{s}$. Since the radius of the ϕ meson is 0.4

fm [32] twice the radius of the J/Ψ meson, $\alpha = 1.25$ is a rather conservative coupling constant to use for the ϕ-N interaction. Also, the interaction is expected to have longer range for the ϕ-N system than that of the $c\bar{c}$-N interaction. Thus, $\mu = 0.6$ GeV used in the variational approach described above is also conservative for the ϕ-N interaction. Further, this attractive force is enhanced inside the nucleus in the quasifree subthreshold photoproduction kinematics.

Experimentally, it is possible to observe the formation of a bound state ϕ-N in the subthreshold quasifree ϕ photoproduction process. The incoming photon couples to a moving nucleon inside the nucleus. The ϕ meson can be produced near rest inside the nuclear medium in the laboratory frame when the initial nucleon is moving in a direction opposite to that of the incoming photon. The attractive QCD van der Waals force between the ϕ meson and nucleons inside the residual nuclear system enhances the probability for the formation of the ϕ-N bound state. It is thus possible for a bound state ϕ-N to be formed inside the nucleus in the quasifree subthreshold ϕ production process from a nuclear target. The experimental search for such a bound state would be a triple coincidence detection of kinematically correlated K^+, K^-, and proton in the final state. The momentum distributions of these final state particles are different from those from unbound quasi-free ϕ production and the direct quasifree K^+K^- production. Thus, it is possible to identify a bound ϕ-N state experimentally using the above mentioned triple coincidence measurement. Such an experiment is feasible [33] at Jefferson Laboratory where advantages of the continuous-wave electron beam, high luminosity, and the state-of-the-art detector package will be utilized to their full capabilities.

5 Proposed Analyses

Recently, high statistics photoproduction data have been taken by CLAS (g10 and g11) in support of the search for the exotic θ^+ pentaquark state. Such a large sample of data allows the analysis of multiple topologies, including triple coincidence events of K^+, K^-, and proton. Therefore, it is ideal to use the deuterium data sample from g10 to investigate ϕ meson production. Such a study, together with high statistic study of near threshold ϕ production from g11 hydrogen data, will provide the opportunity for new analysis. Table 1 lists all the proposed analysis topologies and the physics associated with each analysis. Preliminary analyses are described below.

Data Set	Target	Analysis topology	Physics
g10/g11	LH_2	pK^+K^- pK^+	near threshold ϕ production
g10	LD_2	K^+K^- pK^+	coherent ϕ production from deuteron
g10	LD_2	pK^+K^-	subthreshold ϕ production
g10	LD_2	pK^+K^-	near threshold quasifree ϕ production

Table 1: Analysis topology for the proposed analysis.

5.1 Production on hydrogen

For both the g10 and g11 running, two-charged particle triggers were used. We propose the analysis of two topologies to study the $\gamma p \to p\phi$ process. Namely, we will study the following 2 final states as shown in Table 1: $pK^+K^-$and pK^+. The combination of these two topologies will give complete coverage of the kinematic space and provide a systematic check of the cross section due to their different acceptances. If the manpower is available, the K^+K^- and pK^- modes could also be measured, however, they are not vital to the physics output.

Figures 7, 8, and 9 demonstrate the acceptance of CLAS for the pK^+, pK^-, and pK^+K^- modes from a hydrogen target. The lower left panel shows the two-dimensional plot of the photon energy versus t for the reconstructed ϕ events, and the lower right spectrum is the reconstructed ϕ events versus the photon energy. It is apparent that when detecting two positive particles, the CLAS acceptance is larger and more forward peaked (smaller $|t|$) than when requiring a negative particle. This is due to the magnetic field setting of positive particles bending outward.

Figure 8 shows the corresponding spectra when the coincidence pK^- events are analyzed. One can clearly see that the acceptance in t is no longer forward peaked. Adding a third (positive) particle in coincidence does not change the kinematic coverage, but reduces the overall acceptance as shown in figure 9.

Despite its low acceptance, using the pK^+K^- mode has advantages. It is kinematically complete and will be used to check the detector calibrations and kinematic fitting procedure. Additionally, it is free of the background $\gamma p \to \Sigma^+ K^+ \pi^- (\Sigma^+ \to p + \pi^0)$ that is present when one detects only positive particles ($M(\pi^- + \pi^0) \approx M(K^-)$).

The statistics of g11 will allow for bins $50MeV$ wide in photon energy and $0.1(GeV/c)^2$ in four momentum transfer $|t|$. This is half the bin size of the g1c analysis in photon energy while still reducing the expected error by a factor of two. The coverage and expected error from this measurement is show on figure 2.

5.2 Coherent production on deuterium

Results from a first look at coherent ϕ production from deuterium from g10 is shown in figure 10. (See the caption for a description of each plot.) In the case of the deuterium target, the photon energy threshold for coherent $\gamma d \to \phi d$ process is 1.297 GeV, much lower than the free production threshold from a nucleon target. The coherent $\gamma d \to d\phi^0$ events are plotted as a function of the tagged photon energy (for E_γ less than 2.0 GeV only) in the lower left panel. The bottom right plot represents the exciting physics result of the measurement - a first ever $|t|$ distribution of the coherent production process. The error bars are statistical only.

The data is from the entire high-field running of g10 using the K^+K^- mode. There is an equal amount of data from the low field setting that will double the statistic of this mode. Additionally, we will measure coherent production from the dK^+ mode. From the improved acceptance from the detection of only positive particles, in addition to another statistics boost, we will gain more events in the low $|t|$ region as demonstrated in Figure 11. Thus, the combined analysis of K^+K^- and dK^+ will provide access to kinematics where either single or double scattering occurs. Additionally, as with the hydrogen analysis, a comparison of two topologies with different acceptances will allow for systematic checks of our calculations.

It should be noted that this analysis also shares analysis interests with Jefferson Lab E05-011, the measurement of the coherent vector meson production off the deuteron [25] which was proposed to measure photo- and electro-production of vector mesons (ρ, ω, ϕ) to study the color transparency effect. This proposal was initially approved in 2002, but was deferred under jeopardy in 2005. The physics proposed in the note is significantly distinct from E05-011 and, and the authors feel that the analysis performed under this CAA will benefit E05-011 as well.

5.3 Sub-threshold ϕ meson production from deuterium from g10 data set

We will study the quasifree $\gamma d \to pK^+K^-(n)$ process both above and below the free nucleon production threshold. The requirement of the triple coincidence detection of a

proton and two charged kaons allows the separation of these processes from coherent production by the reconstruction of the spectator nucleon in the case of a deuterium target. The quasifree production cross-section will be extracted as a function of momentum transfer $|t|$. The comparison between the extracted cross-section and the model cross-section based on the nucleon momentum distribution inside the deuteron and the above threshold production cross-section, provides a cross check of our understanding of the quasifree ϕ production process. Such a study is important for the understanding of the sub-threshold production mechanism (and coherent production). We will also extract the sub-thresold production cross-section to compare with the prediction based on the nucleon momentum distribution inside the deuteron and the near threshold ϕ meson production from hydrogen. Such a comparison will be important in making predictions for subthresold ϕ production from heavier nuclear targets in order to search for the ϕ-N bound state in the future.

Fig. 12 shows two-dimensional plot of photon energy versus the invariant mass of the K^+K^- particles from triple concidence detection of pK^+K^- particles. The left panel shows the result from a hydrogen target and the middle panel is the result from the deuterium target. For comparison, the Monte Carlo simulation result for deuterium is shown in the right panel. The ϕ meson events from both targets are clearly shown in these spectra. Fig. 13 shows the invariant mass spectra of the K^+K^- particles with a photon energy cut of great than 1.75 GeV for both the hydrogen (left) and the deuterium target (middle). The simulated result for deuterium is shown in the right panel.

The physical threshold for the $\gamma N \rightarrow \phi N$ is 1.57 GeV. However, due to the limitation of the CLAS acceptance for detecting the three-charged-particle (proton, K^+ and K^-) final state, the acceptance weighted threshold is around 1.75 GeV. Fig. 9 shows various spectra from triple coincidence detection of the K^+,K^-, and proton from the g10 hydrogen data set. The lower left panel shows the two-dimensional plot of the photon energy versus t for the reconstructed ϕ events, and the lower right spectrum is the reconstructed ϕ events versus the photon energy. One can see clearly that the CLAS acceptance weighted threshold for ϕ production from the proton is around 1.75 GeV. Fig. 14 shows the corresponding spectra for a photon energy cut of less than 1.75 GeV. As expected, there is no observation of ϕ events from a proton target for photon energies below 1.75 GeV, while there are events in the deuteron case from the subthresold production of ϕ. The Monte Carlo simulation [1] which takes into account the nucleon momentum distribution inside the deuteron is shown in the right panel. The deuterium spectrum shown in Fig. 14 represents the entire g10 D2 low field data set. The final statistics will be improved by a factor of two once the high field data are included.

This preliminary study shows that the "sub-threshold" production cross-section is very small especially in the deuteron case as one expects. Heavier nuclear targets will enhance the subthresold production events due to larger number of nucleons inside the nucleus, and the larger Fermi momentum distribution.

[1] The events simulated have not been weighted by the differential cross-section.

6 Collaboration and Manpower

The collaboration has extensive experience with photoproduction of mesons. The South Carolina group has been very active in g10 and g11 data anlysis for the pentaquark searches, and in the analysis of CLAS ϕ meson photoproduction. The Duke Medium Energy Physics group has been active in studies of deuteron photodisintegration and photopion production in Hall A and Hall C. Currently, the group is engaged in a CLAS Approved Analysis on pion photoproduction using the g10 data. Additionally, T. Mibe of Ohio University is an expert in ϕ meson studies (his Ph.D. thesis is on *phi* production from SPring-8). [12] The proposed analysis will have student and postdoc involvement from both South Carolina and Duke University. The collaboration has sufficient manpower and expertise to carry out the proposed analysis.

References

[1] N. Isgur and M.B. Wise, Phys. Lett. B **232**, 113 (1989); 237, 527 (1990).

[2] E. Anciant *et al.*, Phys. Rev. Lett. **85**, 4682 (2000).

[3] T. H. Bauer, R. D. Spital, D. R. Yennie, and F. M. Pipkin, Rev. Mod. Phys. **50**, 261 (1978); *ibid* **51**, 407(E) (1979); D. G. Cassel *et al.*, Phys. Rev. **D24**, 2787 (1981).

[4] D.P. Barber *et al.*, Z. Phys. **C12**, 1 (1982).

[5] H.-J. Behrend *et al.*, Nucl. Phys. **B144**,22 (1978).

[6] H.J. Betsch,*et al.*, Nuc. Phys. **B70**, 257 (1974);

[7] J. Ballam *et al.*, Phys. Rev. **D7**, 3150 (1973).

[8] H.J. Halpern , Phys. Rev. Lett. **29**, 1425 (1972).

[9] A.I. Titov *et al.*, Phys. Rev. C **60**, 035205 (1999); Y. Oh *et al.*, Phys. Lett. **B 462**, 23 (1999); A.I. Titov, private communication.

[10] Q. Zhao, J.-P. Didelez, M. Guidal, and B. Saghai, Nucl. Phys. **A660**, 323 (1999). Q. Zhao, B. Saghai, and J.S. Al-khalili, Phys. Lett. B **509**, 231 (2001).

[11] D. Tedeschi *et al.*, "Electromagnetic Interactions in Nuclear and Hadronic Physics", M. Fujiwara and T. Shima (Eds.), World Scientific, 367 (2002).

[12] T. Mibe *et al.*, arXiv:nucl-ex/0506015.

[13] J. Barth, *et al.*, Eur. Phys. J. A**17**, 269-274 (2003).

[14] J.-M. Laget, hep-ph/0003213(2000).
J.-M. Laget, R. Mendez-Galain, Nucl. Phys.**A581**, 397 (1995). Private communication.

[15] M. Pichowsky and T.-S. H. Lee, Phys. Rev. **D56**, 1644 (1997).

[16] R.A. Williams, Phys. Rev. **C57**, 223 (1998).

[17] H.-J. Behrend, et al., Phys. Lett. B **56**, 409 (1975)

[18] T. Ishikawa, et al., Phys. Lett. B **668**, 215 (2005)

[19] E. Oset, et al., nucl-th/0504033

[20] L. Frankfurt, et al., Nucl. Phys. **A622**, 511 (1997); L. Frankfurt, et al., Eur. Phys. J. A **2**, 301 (1998)

[21] I.D. Overman, Ph.D. thesis, SLAC-140, UC-34 (1971)

[22] R.L. Anderson, et al., Phys. Rev. D **4** 3245 (1971)

[23] G. McClellan, et al., Phys. Rev. Lett. **26**, 1593 (1971)

[24] A. I. Titov, et al., Phys. Rev. C **66**, 022202(R) (2002)

[25] L.H. Kramer, S. Stepanyan, et al., E02-012 renamed E05-011, approved by Jefferson Lab PAC 21(2002) but deferred under jeopardy by PAC 27 (2005). See http://www.jlab.org/exp_prog/PACpage/PAC27/PAC27_report.pdf.

[26] S. J. Brodsky, I. A. Schmidt and G. F. de Teramond, Phys. Rev. Lett. **64**, 1011 (1990).

[27] M. Luke, A. V. Manohar and M. J. Savage, Phys. Lett. **B288**, 355 (1992) [hep-ph/9204219].

[28] G. R. Court *et al.*, P," Phys. Rev. Lett. **57**, 507 (1986).

[29] S. J. Brodsky and G. F. de Teramond, Proton-Proton Scattering," Phys. Rev. Lett. **60**, 1924 (1988).

[30] A. Donnachie and P.V. Landshoff, Nucl. Phys. **B244**, 322 (1984).

[31] D.A. Wasson, Phys. Rev. Lett. **67**, 2237 (1991).

[32] B. Povh and J. Hüfner, Phys. Rev. Lett. **58**, 1612 (1987).

[33] H. Gao, T.-S.H. Lee, and V. Marinov, Phys. Rev. C **63**, 022201R (2001).

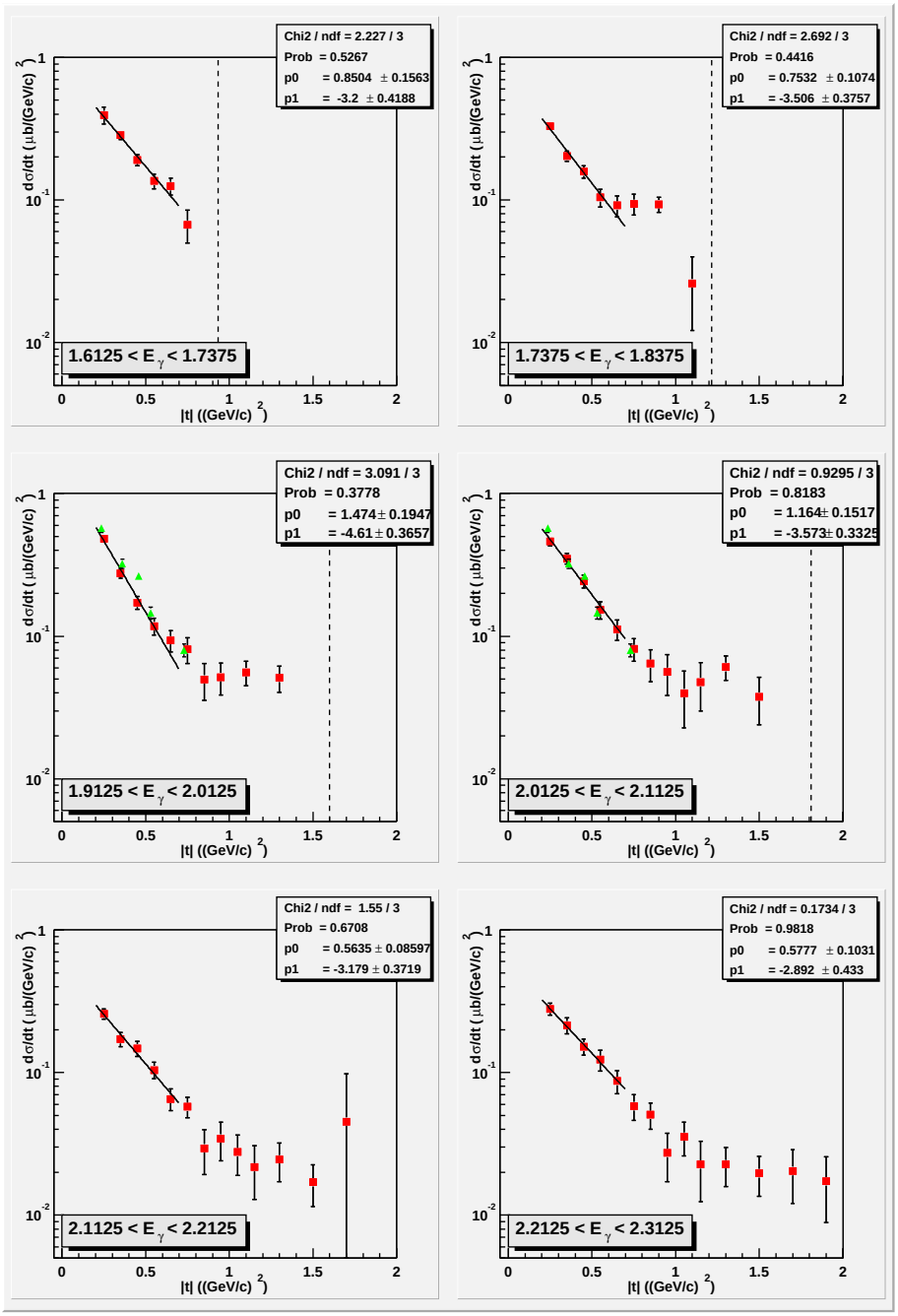

Figure 1: CLAS g1c ϕ production cross sections (red points). The green squares are data from reference [6]. The solid line is an exponential fit of the form $p0exp(p1 * t)$. The parameters p0 and p1 are shown in the figure.The error bars on the CLAS data include statistics from the data and Monte Carlo.

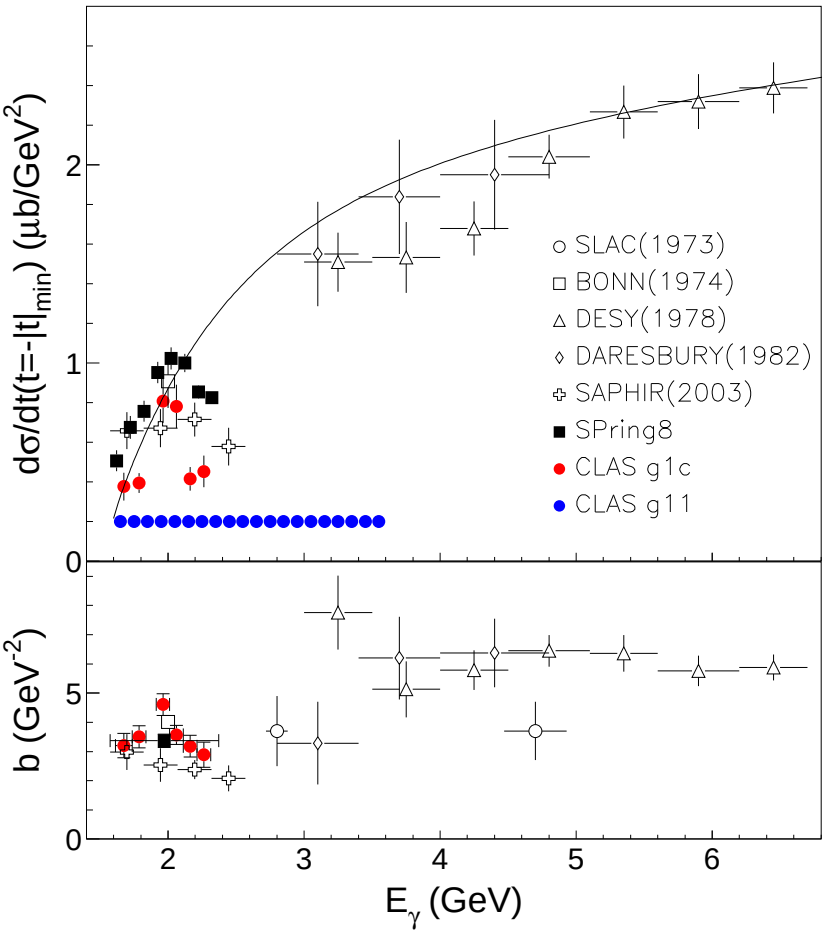

Figure 2: Cross section ($t = |t|_{min}$) and slope parameter for ϕ protoproduction as a function of photon beam energy. The red points are the CLAS g1c data, the crosses are the data from SAPHIR[13], and the black squares are the LEPS data.[12] The solid blue points indicate the coverage and expected errors from the proposed g11 analysis.

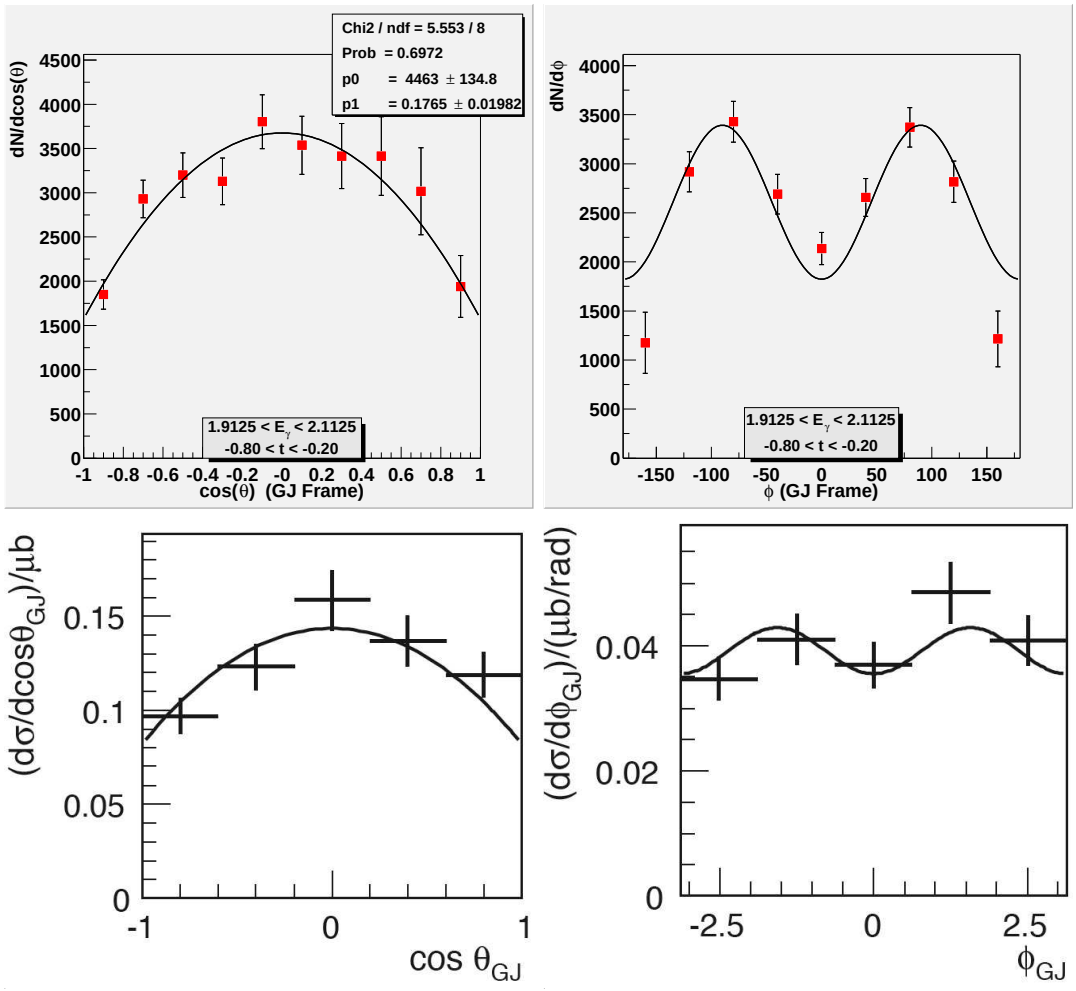

Figure 3: Polar and azimuthal decay distributions for the ϕ meson in the Gottfried-Jackson frame. The upper plots are from the CLAS g1c analysis where the photon energy is $1.9 \leq E_\gamma \leq 2.1$ GeV and the momentum transfer bin is $-0.8 \leq t \leq -0.2$ $(GeV/c)^2$. The lower plots are from SAPHIR[13] where the photon energy range is $1.57 \leq E_\gamma \leq 2.57$ GeV .

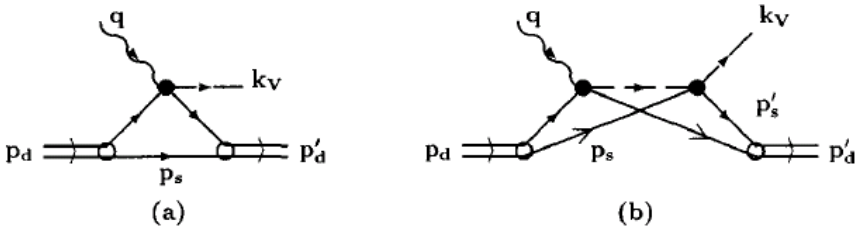

Figure 4: Single scattering (a) and double scattering contribution (b) to exclusive vector meson production in photon-deuteron collisions. (figure from Ref. [20])

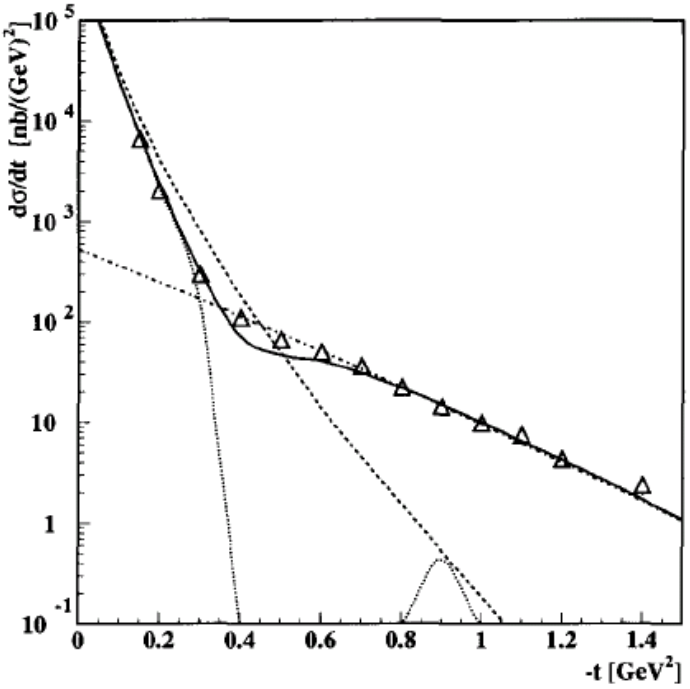

Figure 5: The cross section $d\sigma_{\gamma d\to\rho d}/dt$ for photoproduction of ρ-mesons from unpolarized deuterium. The full curve shows the results of calculation [20] within vector meson dominance. The dashed, dotted and dash-dotted lines account for the Born, Born + interference, and double scattering contribution, respectively. The experimental data are from Ref.[21, 22] taken at a photon energy $E_\gamma = 12$ GeV. (figure from Ref. [20])

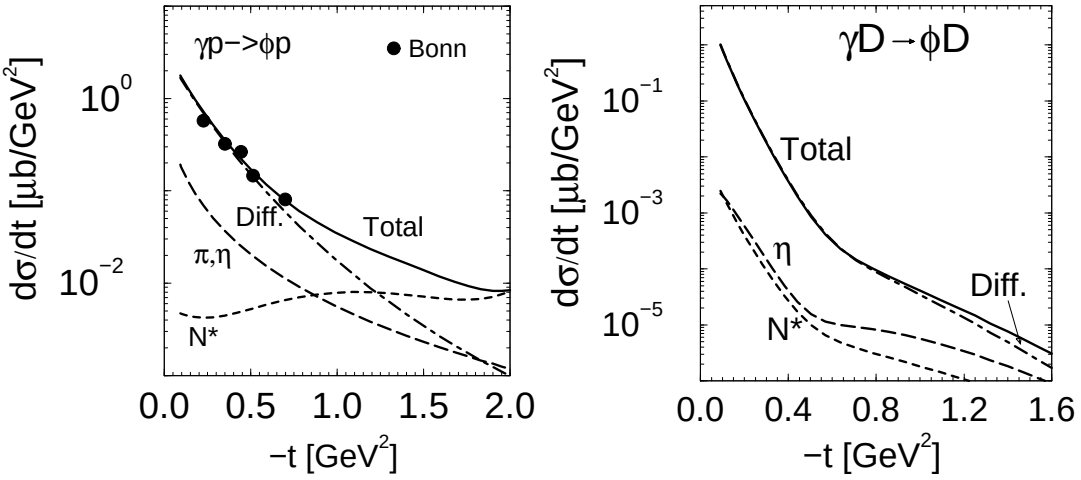

Figure 6: Differential cross sections for the $\gamma p \to \phi p$ (left panel) and $\gamma D \to \phi D$ reactions at $E_\gamma = 2.2$ GeV[24]. Curves represent contributions from diffractive process (Pomeron exchange), π, η-meson exchange and N^* exchange processes. Data are taken from Ref. [6]

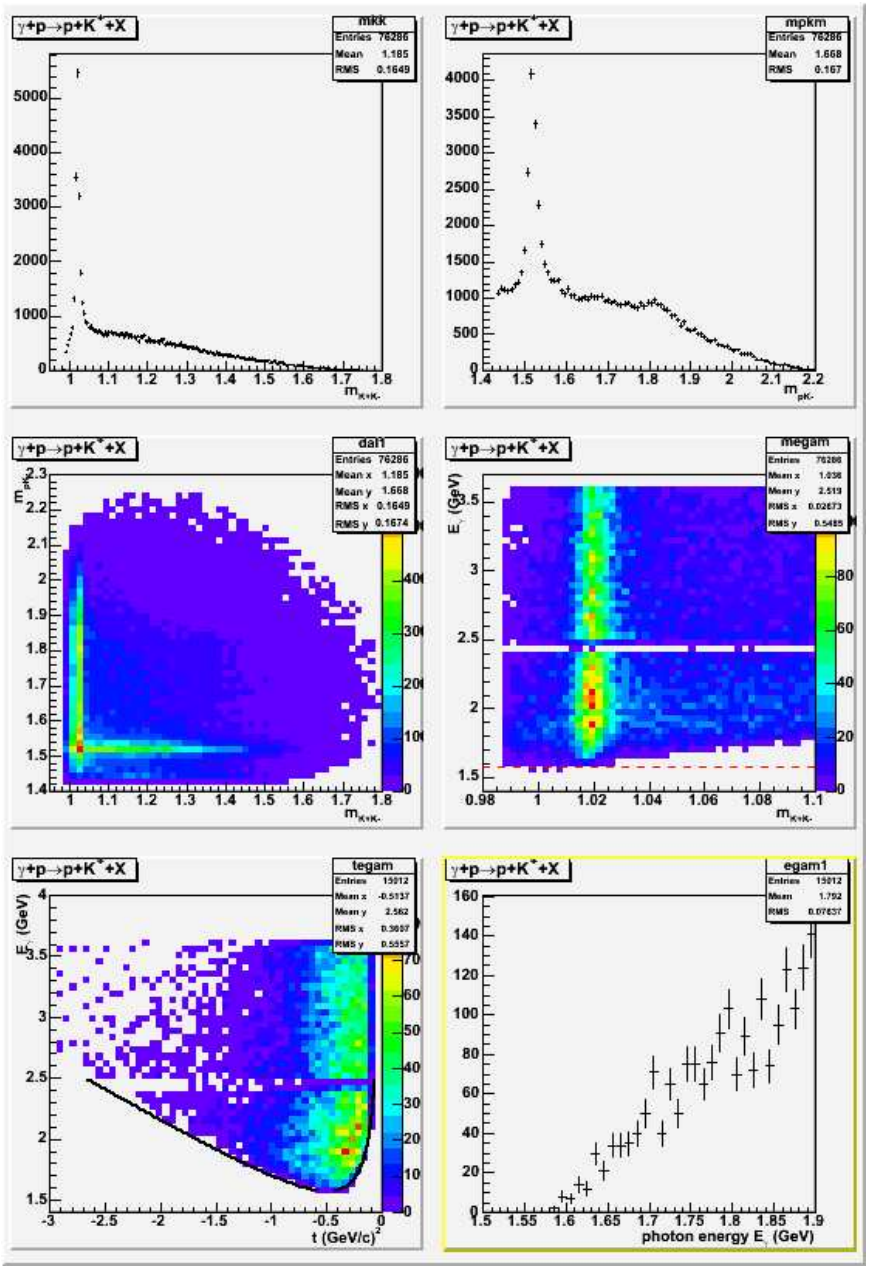

Figure 7: Spectra from coincidence detection of the K^+ and p particles from CLAS g10 hydrogen data. The upper left panel is the invariant mass spectrum from the detected K^+ particle and the reconstructed K^- particle. The upper right panel is the invariant mass spectrum of the proton and the K^+ particle. The middle left panel is the two-dimensional plot of the invariant mass of the K^+p versus K^+K^-, and the middle right panel is the two-dimensional plot of the photon energy versus the invariant mass of the K^+K^- system. The lower left panel is the two-dimensional plot of the photon energy and t for the reconstructed ϕ events, and the lower right panel is the photon energy spectrum for the reconstructed ϕ events.

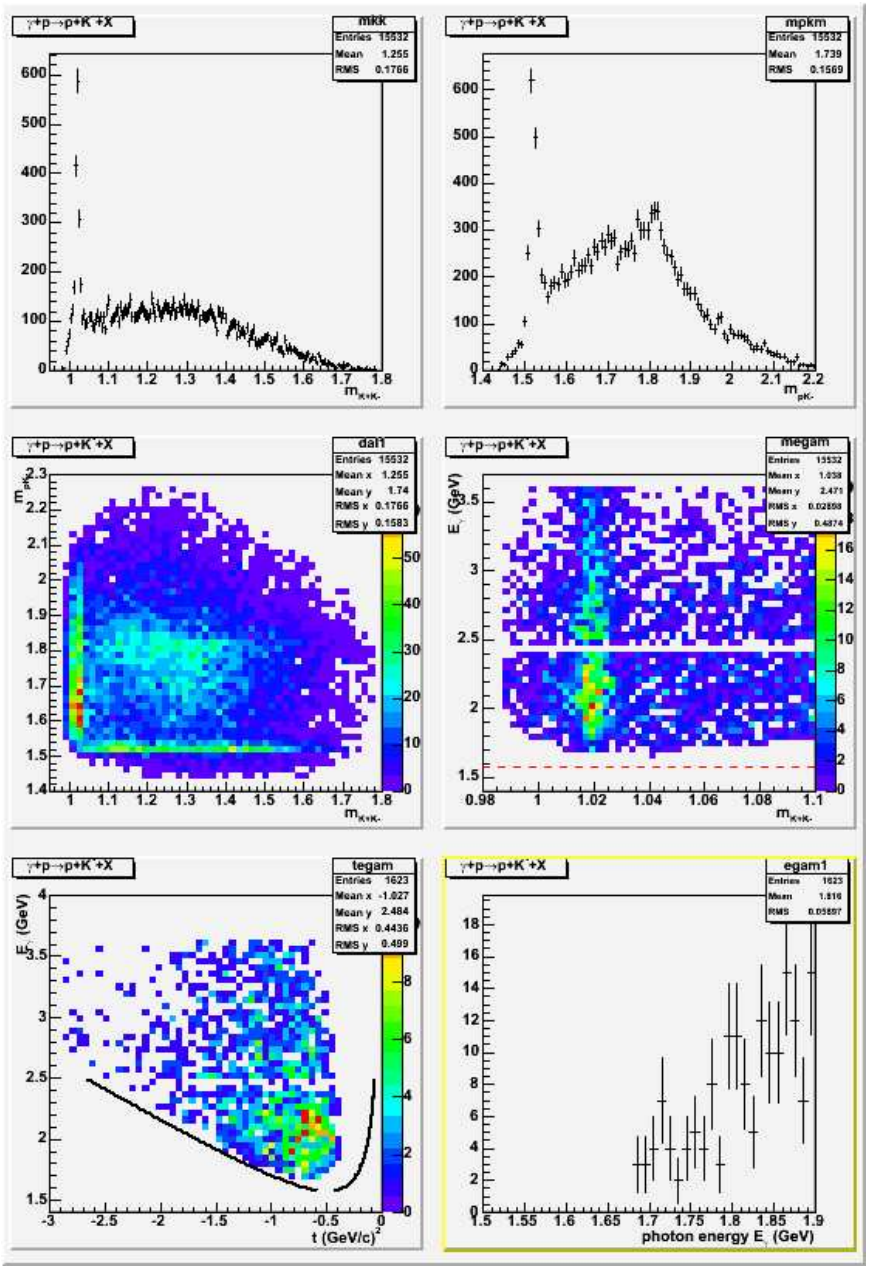

Figure 8: Spectra from coincidence detection of the K^- and p particles from CLAS g10 hydrogen data. The upper left panel is the invariant mass spectrum from the detected K^- particle and the reconstructed K^+ particle. The upper right panel is the invariant mass spectrum of the proton and the K^- particle. The middle left panel is the two-dimensional plot of the invariant mass of the K^-p versus K^+K^-, and the middle right panel is the two-dimensional plot of the photon energy versus the invariant mass of the K^+K^- system. The lower left panel is the two-dimensional plot of the photon energy and t for the reconstructed ϕ events, and the lower right panel is the photon energy spectrum for the reconstructed ϕ events.

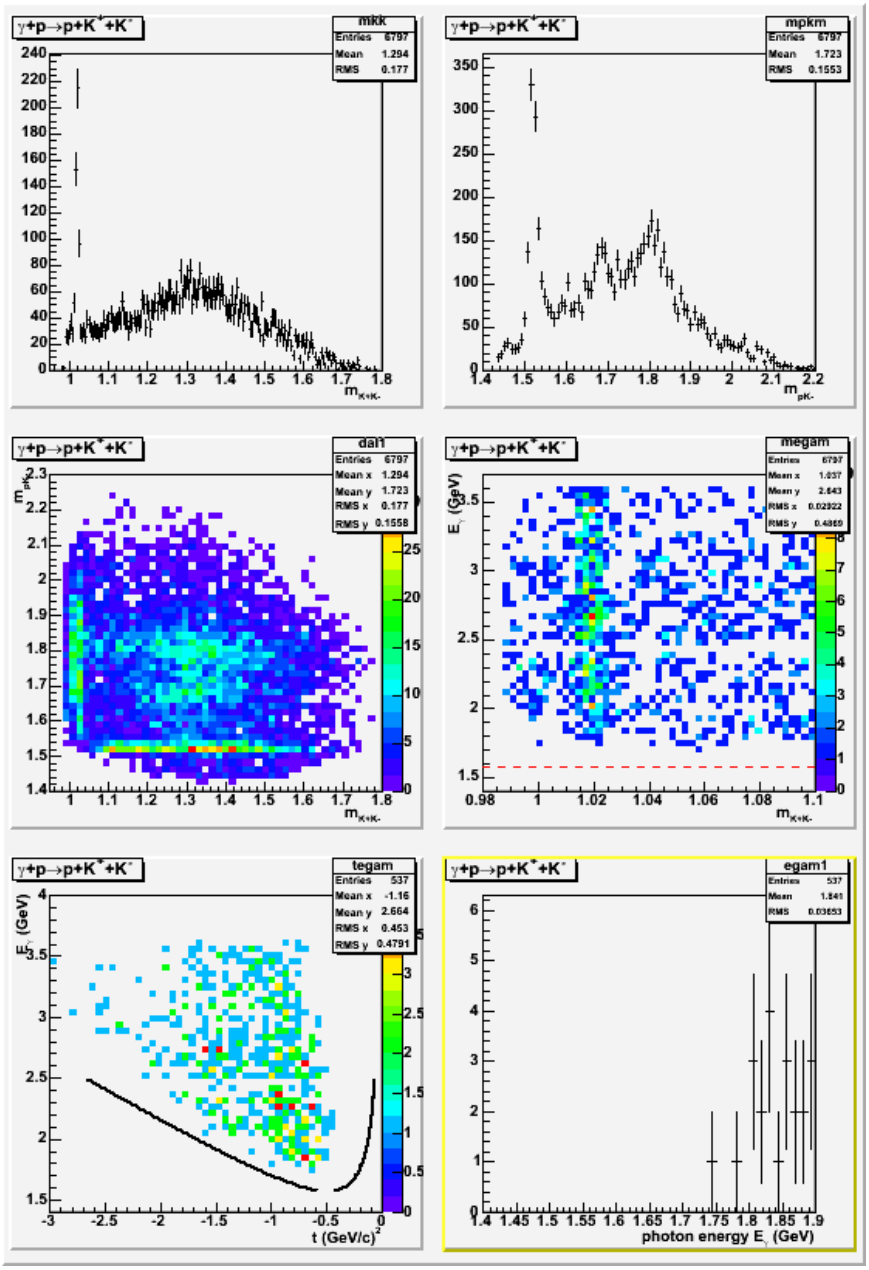

Figure 9: Spectra from triple coincidence detection of the K^+K^-p particles from CLAS g10 hydrogen data. The upper left panel is the invariant mass spectrum of the K^+ particle and the K^- particle. The upper right panel is the invariant mass spectrum of the proton and the K^+ particle. The middle left panel is the two-dimensional plot of the invariant mass of the K^+p versus K^+K^-, and the middle right panel is the two-dimensional plot of the photon energy versus the invariant mass of the K^+K^- system. The lower left panel is the two-dimensional plot of the photon energy and t for the reconstructed ϕ events, and the lower right panel is the photon energy spectrum for the reconstructed ϕ events.

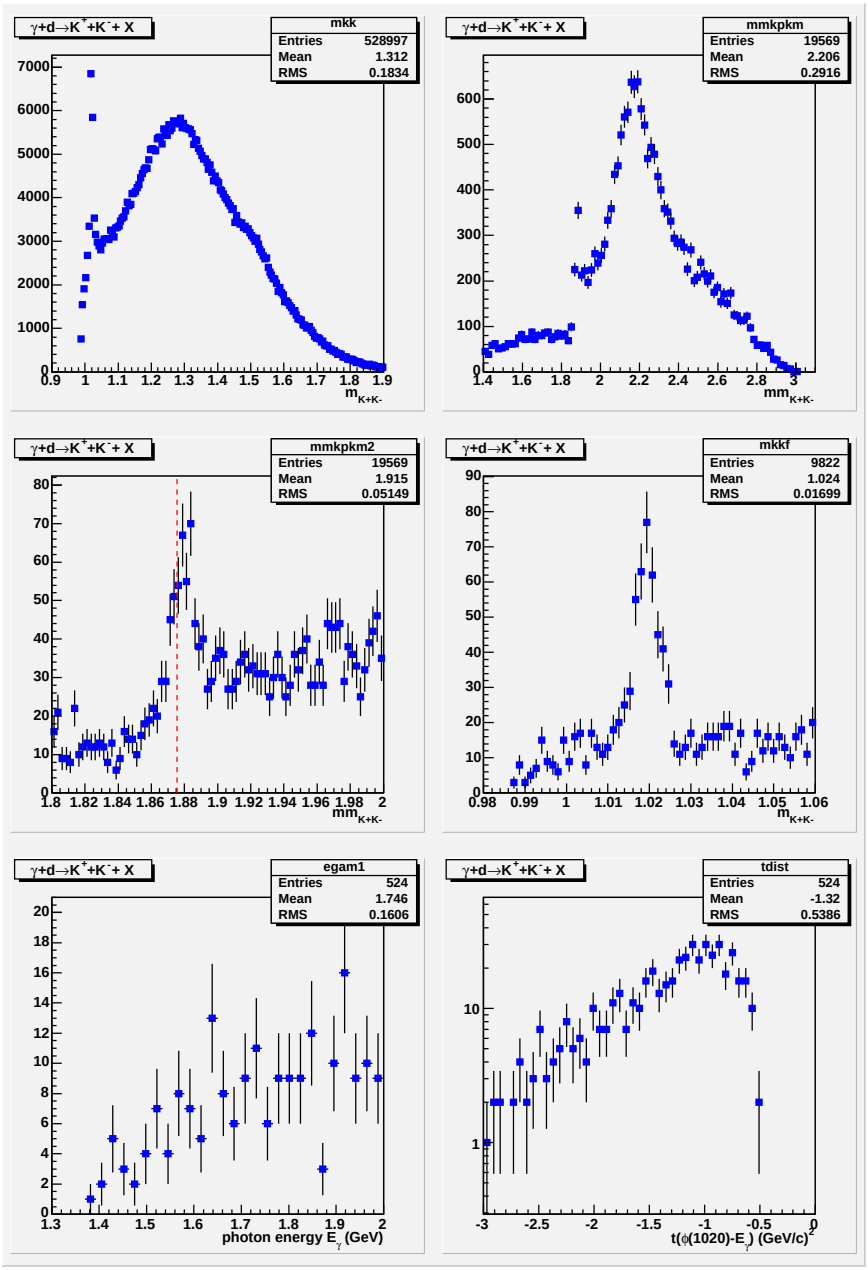

Figure 10: Spectra from coincidence detection of the K^+K^- particles from CLAS g10 deuterium data (high field). Top left: K^+K^- invariant mass. Top right: K^+K^- missing mass. Middle left: K^+K^- missing mass with invariant mass cut around phi mass. The dotted line indicates the deuteron mass. Middle right: K^+K^- invariant mass with missing mass cut around the deuteron mass. Lower left: Photon energy distribution with combined invariant mass and missing mass cuts. Lower right: $|t|$ distribution with combined invariant mass and missing mass cuts.

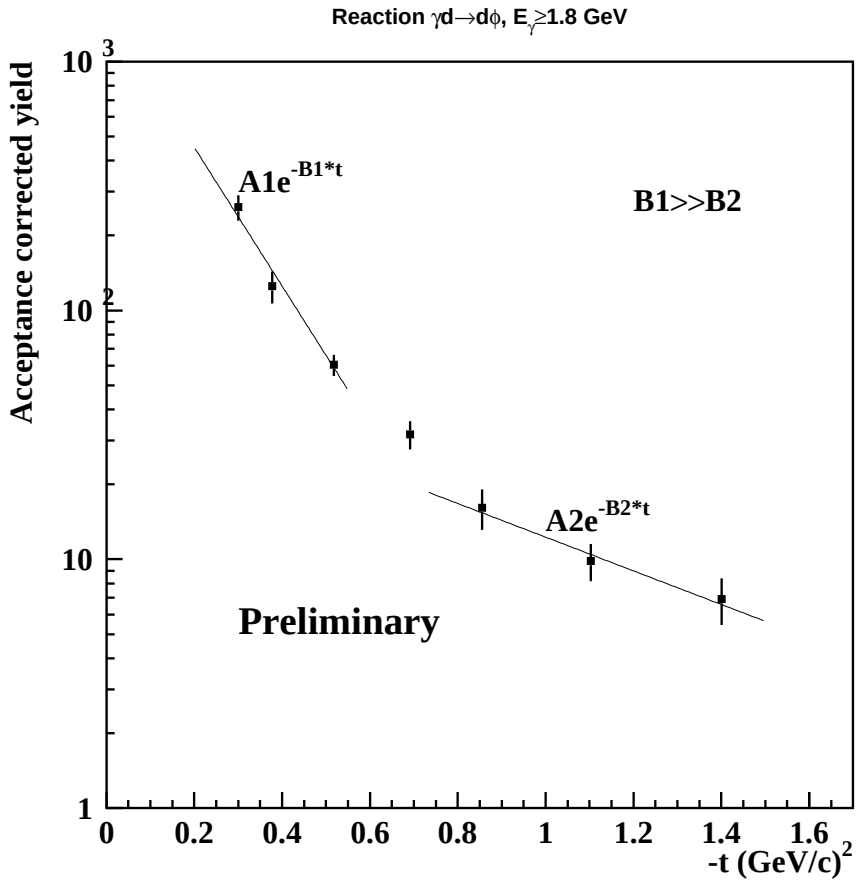

Figure 11: Cross section from coincidence detection of the dK^+ particles from CLAS g2a data set.

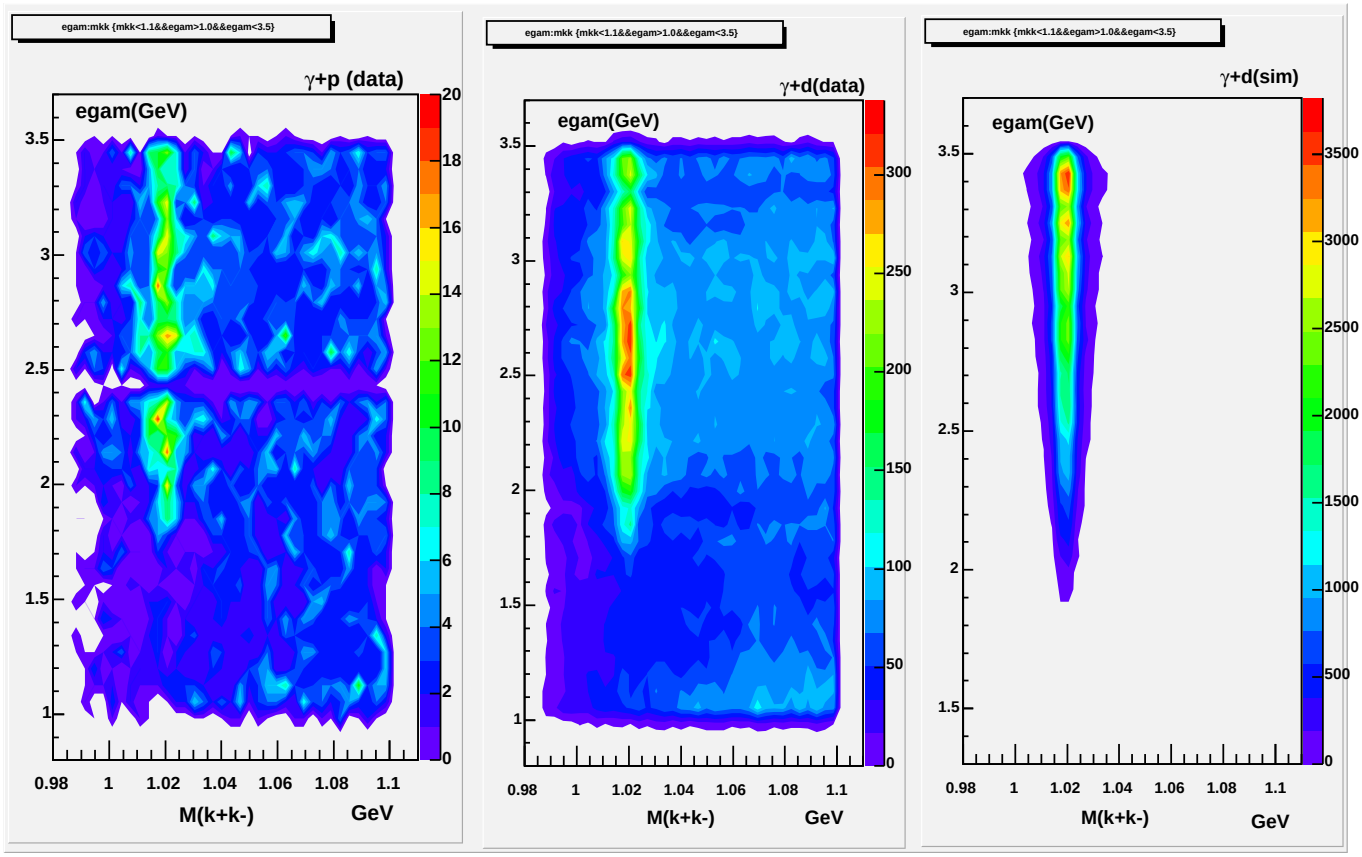

Figure 12: Two dimensional spectra from CLAS g10 data on the photon energy E_γ (vertical) in GeV versus the invariant mass of K^-K^+ (horizontal) in GeV. The left panel is from the hydrogen target, the middle panel is from the deuterium target, and the right panel is from simulation (see text for details).

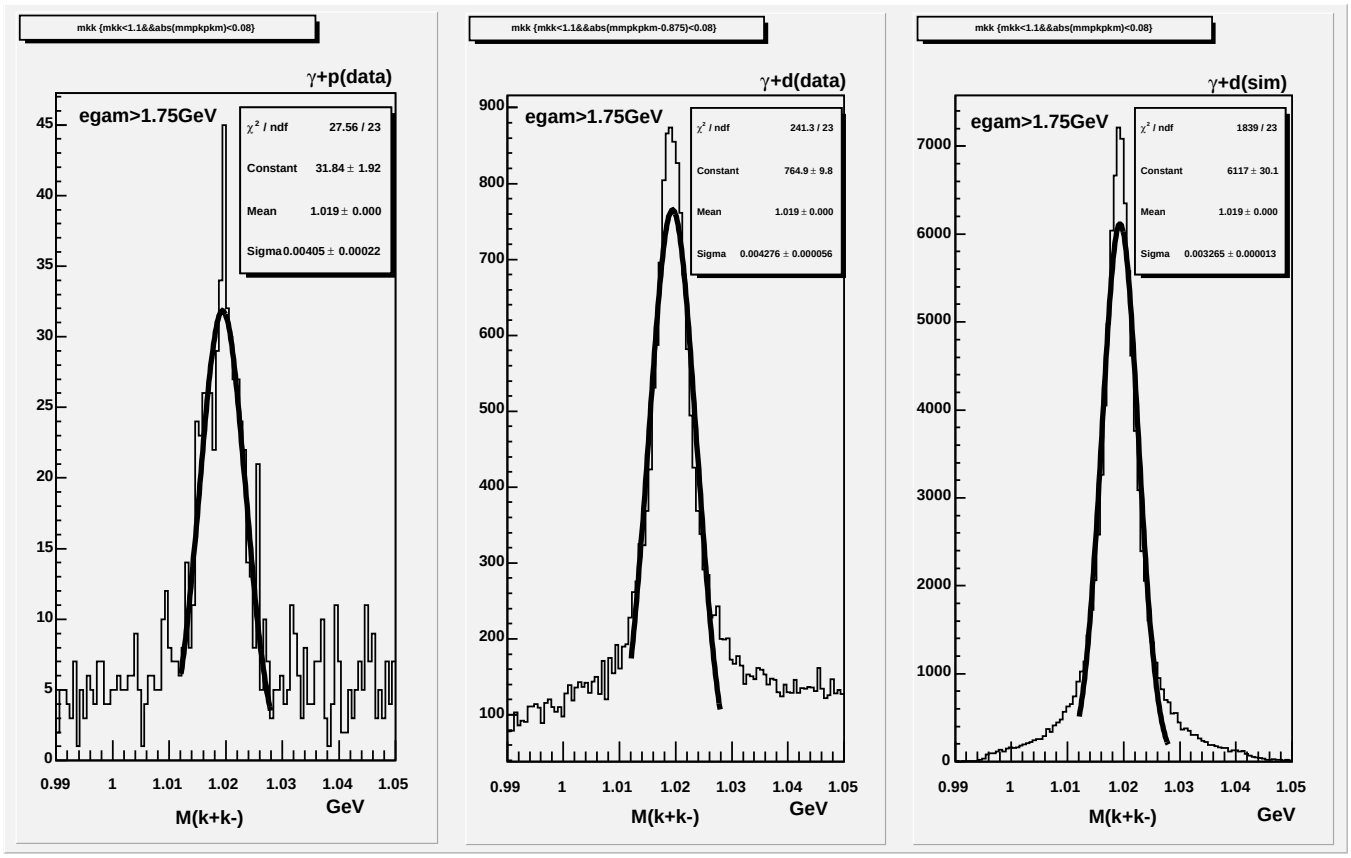

Figure 13: Invariant mass spectra (in GeV) of K^-K^+ particles from triple coincidence detection of the K^+K^-p particles from CLAS g10 data. The left panel is from the hydrogen target, the middle panel is from the deuterium target, and the right panel is from simulation. A cut which requires the photon energy to be greater than 1.75 GeV was applied in this analysis.

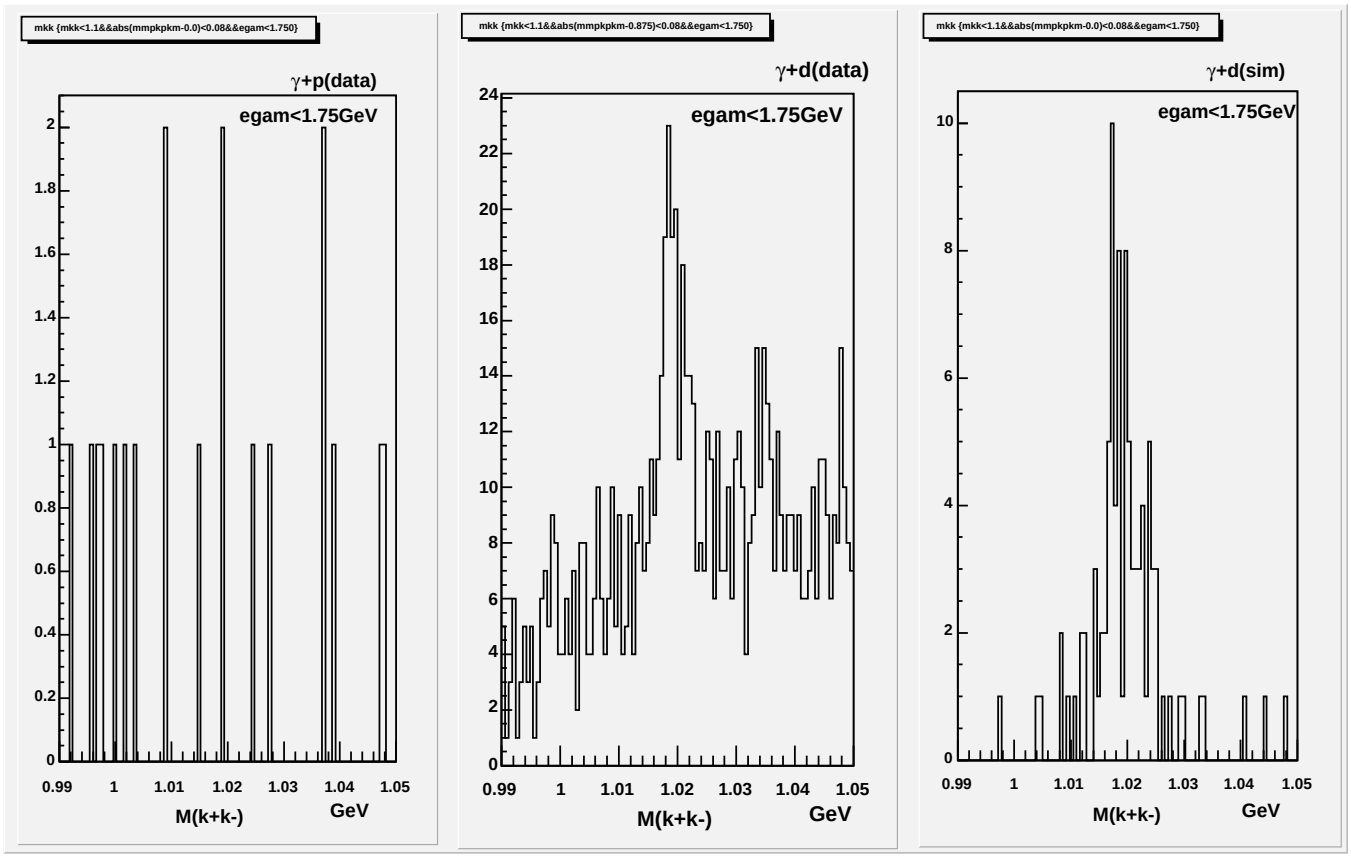

Figure 14: Invariant mass spectra (in GeV) of K^-K^+ particles from triple coincidence detection of the K^+K^-p particles from CLAS g10 data. The left panel is from the hydrogen target, the middle panel is from the deuterium target, and the right panel is from the simulation. A cut which requires the photon energy to be less than 1.75 GeV was applied in this analysis.

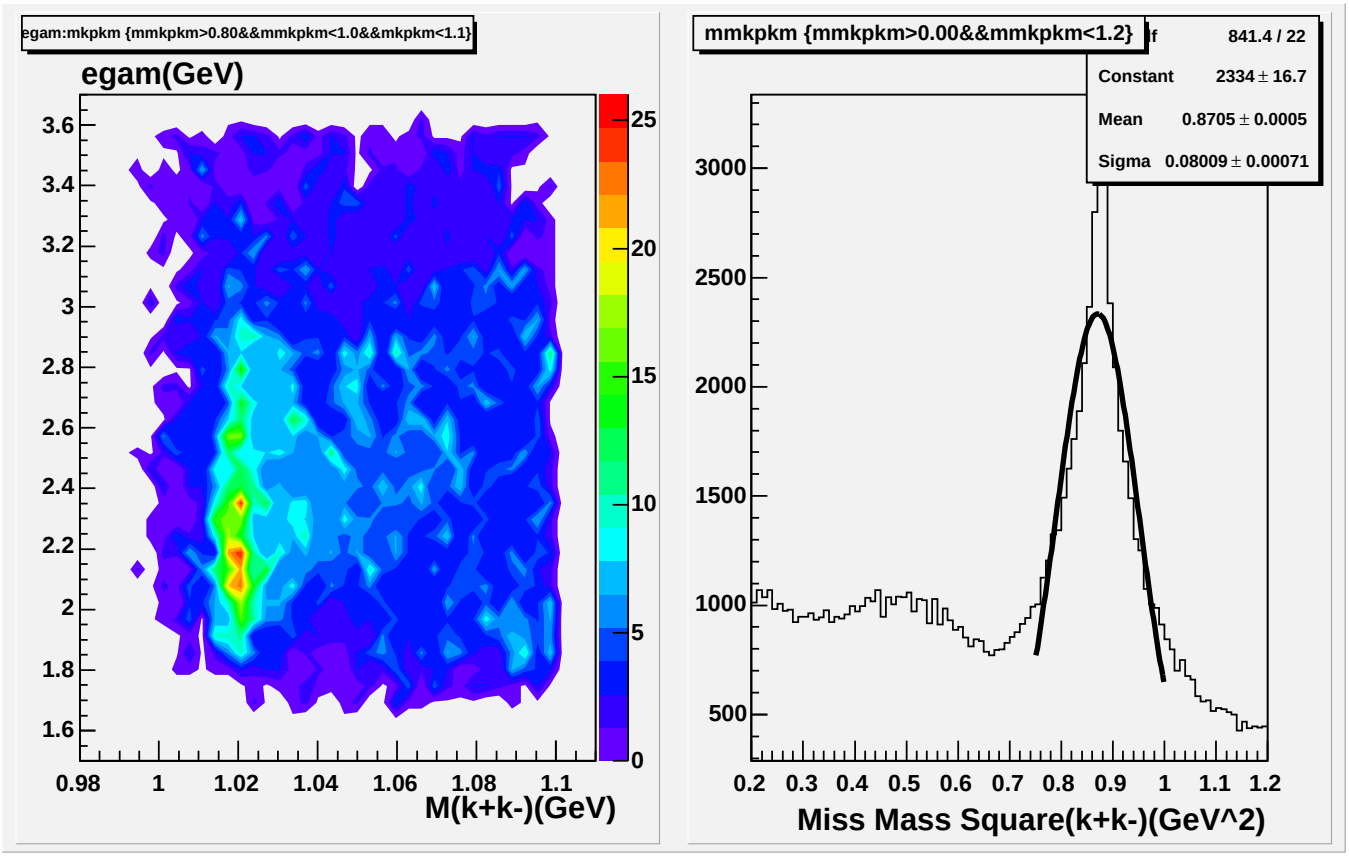

Figure 15: Spectra from coincidence detection of the K^+K^- particles from CLAS g10 hydrogen data. The left panel is the photon energy E_γ (vertical) in GeV versus the invariant mass of K^-K^+ (horizontal) in GeV. The right panel is the missing mass squared plot from detecting the K^+K^- particles in coincidence.